



Room temperature electrosynthesis of ZnSe thin films

Y.G. Gudage, N.G. Deshpande, Abhay A. Sagade, Ramphal Sharma*

Thin film and Nanotechnology Laboratory, Department of Physics, Dr. B.A.M. University, Aurangabad 431004 (M.S.), India

ARTICLE INFO

Article history:

Received 13 July 2008

Received in revised form 1 November 2008

Accepted 5 November 2008

Available online 17 November 2008

Keywords:

Electrosynthesis

ZnSe

X-ray diffraction

Cubic phase

Atomic force microscopy

ABSTRACT

In the present study, we report the room temperature electrosynthesis of Zinc selenide (ZnSe) thin films on stainless steel (SS) and fluorine doped tin oxide (FTO) coated glass substrates. In addition, the influence of the substrate on the microstructural properties of ZnSe is plausibly explained. Voltammetric curves were recorded in order to characterize the electrochemical behaviour of $\text{Zn}^{2+}/\text{SeO}_2$ system. The as-deposited ZnSe thin films have been characterized for structural (X-ray diffraction (XRD)), surface morphological (scanning electron microscopy (SEM)), compositional (energy dispersive analysis by X-rays (EDAX)), surface topographical (atomic force microscopy (AFM)) and optical absorption analysis. Formation of cubic structure with preferential orientation along the (1 1 1) plane was confirmed from structural analysis. A significant observation seen from the SEM micrograph was the formation of porous layer on the FTO coated glass substrate. However, this is not seen in case of stainless steel substrate. Similar observation was predicted in case of AFM analysis for the films deposited on FTO. The optical band gap for ZnSe thin films was found to be 2.7 eV.

© 2008 Elsevier B.V. All rights reserved.

1. Introduction

Synthesis and characterization of wide gap II–VI semiconductors are of great importance, since these materials can be utilized in a variety of optoelectronic applications, viz. solar cells, heterojunction LED, photoconductors, etc. Though Zinc selenide (ZnSe) has a direct wide band gap (2.7 eV) it is exceptionally interesting material for the applications like optoelectronics, especially for fabrication of the blue light diodes, also it acts as a buffer/window layer in chalcogenide-based thin film solar cells (by constructing a heterojunction under lattice matching conditions) [1–3].

There are several reports available on the growth of ZnSe thin films by various techniques such as chemical vapour deposition (CVD) [1], screen printing [4], vacuum evaporation [5,6], pulsed laser deposition (PLD) [7], chemical bath deposition (CBD) [8,9], etc. It has been identified that the deposition from aqueous solution makes the process simple, economical and easily scalable. CBD and electrochemical deposition (ECD) are the commonly known popular techniques for the deposition of films from aqueous solution. Several authors have reported on the chemical bath deposition of ZnSe thin films from aqueous solution [9–11]. But, in CBD, the material wastage is high and the control over rate of deposition is rather difficult. Electrodeposition is one of the most widely accepted tech-

niques for the economical and efficient growth of the films from aqueous solution, and numerous reports are available on the deposition of various thin films by this technique. But it is very surprising to note that the electrodeposition of ZnSe thin films has not been studied in comparison with cadmium chalcogenides. Also it is worth to note that electrodeposition of the ZnSe is difficult because of the wide difference in the reduction potential of Zn and Se ions [12], and only few reports are available on the electrodeposition of ZnSe thin films [12–17].

Abundant literature is available on preparation and characterization of ZnSe by using ZnSO_4 and ZnCl_2 as source materials for “ Zn^{2+} ” source [12–18]. Selenious acid has been reported as a “ Se^{2-} ” source by many workers [15,19]. However, no attempt is made on electrosynthesis of the ZnSe by using zinc acetate as a source of Zn^{2+} from aqueous acidic bath. In view of this, an attempt has been made to electrosynthesize ZnSe thin films at different pH of the bath ranging from 2 to 3 at the interval of 0.5. The as-deposited films were studied for structural, surface morphological and optical properties. In addition, the influence of the substrate on the microstructural properties have been studied and compared with the reported literature wherever necessary.

2. Experimental

2.1. Preparation of ZnSe thin films

ZnSe thin films were electrodeposited potentiostatically by a conventional three-electrode set-up. Cyclic voltammetric measurements and the ZnSe electrodeposition were made by using a potentiostat (Princeton PerkinElmer, Applied Research Versa stat II; Model 250/270) in the three-electrode configuration. The cell consists of stainless steel (SS) and/or fluorine doped tin oxide (FTO) coated glass as the working

* Corresponding author at: Inorganic-Nanomaterials Laboratory, Department of Chemistry, Hanyang University, Sungdong-Ku, Haengdang-dong 17, Seoul 133-791, South Korea. Tel.: +82 2 22925212; fax: +82 2 22200762.

E-mail address: rps.phy@gmail.com (R. Sharma).

electrode, graphite as the counter electrode and saturated calomel electrode (SCE, $E_0 = 244$ mV vs SHE, the standard hydrogen electrode) as the reference electrode. The working and counter electrodes were placed parallel to each other separated by a distance of 0.3 cm. The electrolyte solutions were prepared by dissolving $\text{Zn}(\text{CH}_3\text{COO})_2 \cdot 2\text{H}_2\text{O}$ and SeO_2 in double distilled water. The pH of the solution was adjusted by using 1 M H_2SO_4 . The pH of the bath was varied from 2 to 3 at the interval of 0.5. Digital μ -pH meter (Systronics-361) was used to measure the pH of electrolytic bath. Electrodeposition was carried out on the unit area (1 cm^2) of the substrates in potentiostatic mode at room temperature (27°C) from an unstirred bath. The substrate cleaning process is discussed elsewhere [20]. The as-deposited films of ZnSe were further studied for various properties.

2.2. Characterization of ZnSe thin film

Thin films of ZnSe were characterized for structural, surface morphological, compositional and optical properties. Thickness of the film was measured by Surface profiler (AMBIO XP-1). The structural analysis of the films were made by an X-ray diffractometer (Bruker AXS, D8 Advance, Germany, CuK_α radiation at $\lambda = 1.5406 \text{ \AA}$) in the 2θ range 20 – 60° . The surface morphology and composition was studied by scanning electron microscopy (SEM) and energy dispersive analysis by X-rays (EDAX) using JEOL-JSM 6360, respectively. An atomic force microscopy (AFM) study was done using Nanoscope IIIa (silicon nitride cantilever; tip radius of 20 nm ; operated in tapping mode) provided by Veeco digital instruments. To study the optical characteristics of the film, absorbance and transmittance spectra were recorded in the range 300 – 1100 nm by means of UV–vis–NIR spectrophotometer (PerkinElmer, Lambda 25).

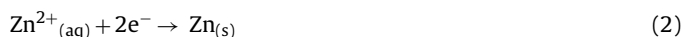
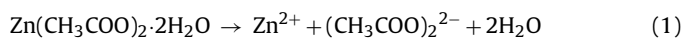
3. Results and discussion

3.1. Voltammogram study

Cyclic voltammetry is the best tool to monitor the electrochemical reactions in precursor solutions and to find the suitable deposition potential range. Fig. 1(a) shows a cyclic voltammogram (scan rate 50 mV/s) of $0.1 \text{ M Zn}(\text{CH}_3\text{COO})_2 \cdot 2\text{H}_2\text{O}$ solution on SS electrode at pH 2.5 of the electrolyte bath. From this figure the reduction potential was found to be -0.8 V vs SCE. Fig. 1(b) shows a cyclic voltammogram of 0.01 M SeO_2 solution on SS electrode at pH 2.5. The curve shows the gradual increase in current with applied potential. So it is not possible to locate the exact deposition potential. At the deposition potential of -0.45 V vs SCE, there is formation of reddish elemental 'Se' on the working electrode.

Fig. 2(a) shows the linear sweep voltammogram (LSV) of $0.1 \text{ M Zn}(\text{CH}_3\text{COO})_2 \cdot 2\text{H}_2\text{O} + 0.01 \text{ M SeO}_2$ solution on SS (at pH 2.0, 2.5 and 3.0) and FTO coated glass (at pH 2.5) electrode. It can be seen, that the overall polarization curves contain two distinct regions: first corresponding to reduction of Se^{2+} to Se and second corresponding to reduction of Zn^{2+} to Zn. These two regions are separated by a very small plateau region (potential independent region), where the electrolysis current is limited by mass transport, in particular by diffusion of chalcogen ions towards the cathode. The as-controlled $\text{Se}(\text{VI})$ and $\text{Zn}(\text{II})$ co-reduction results in the formation of semiconductive ZnSe-containing layers within a potential range of approximately -0.6 to -0.9 V vs SCE. To get the optimum conditions for co-deposition, the deposition potential was suitably chosen so that both the Zn and Se species get deposited uniformly. For stoichiometric deposition of the ZnSe on both the electrodes, the optimum deposition potential was identified to be -0.75 V vs SCE and pH of the bath equal to 2.5.

The electrochemical reaction on the cathode takes place as follows:



On reduction of H_2SeO_3 ,

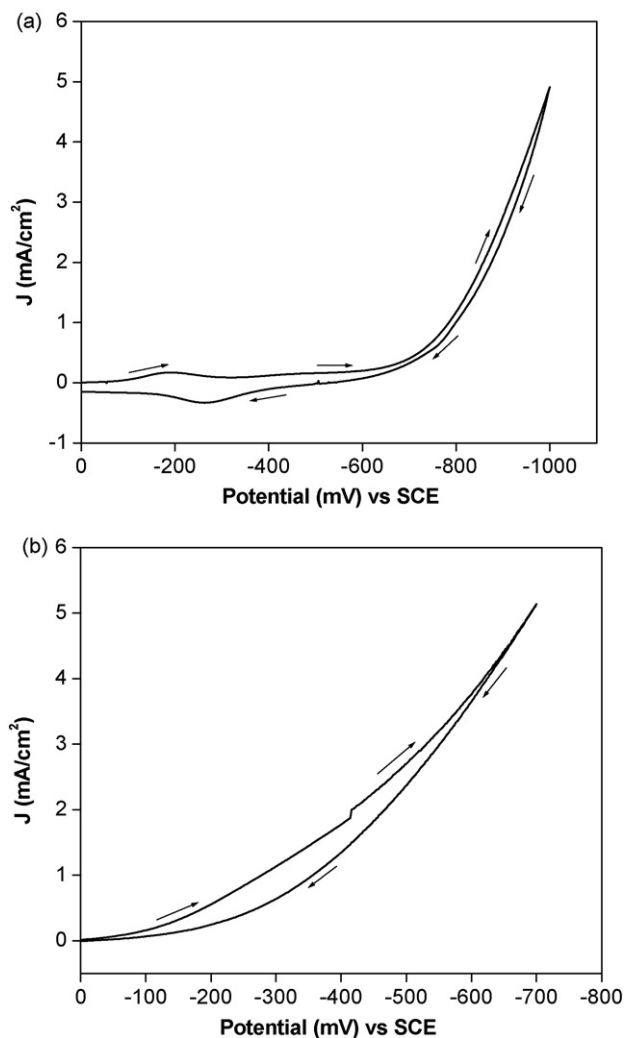
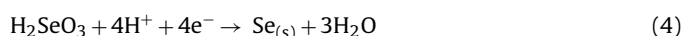


Fig. 1. Cyclic voltammogram of (a) $0.1 \text{ M Zn}(\text{CH}_3\text{COO})_2 \cdot 2\text{H}_2\text{O}$ and (b) 0.01 M SeO_2 solution on stainless steel (SS) electrode at pH 2.5.

The dependence of the current density on the pH of the electrolytic solution containing $0.1 \text{ M Zn}(\text{CH}_3\text{COO})_2 \cdot 2\text{H}_2\text{O} + 0.01 \text{ M SeO}_2$ solution is shown in Fig. 2(b). When pH of the plating solution is 2.0, the current density decreased continuously with time. The films deposited at this pH value were found to have very poor adherence and the deposit dissolves out due to hydrogen evolution at the electrode.

At pH 2.5 of the electrolytic bath, the current density decreases rapidly at first and then gradually stabilizes at a constant value (this behaviour is similar to both working electrodes; Fig. 2(b)). When the electrode potential is applied, there is a sharp rise in the current density at the electrode surface this may be due to formation of the ZnSe nuclei on electrode surface. After an initial surge the current density decreases for longer time revealing the coverage of the ZnSe ions on to the electrode surface. This phenomenon occurs due to formation of the ZnSe nucleus on surface of the substrate, which results in decreasing of the current densities, rapidly. When ZnSe film was covered on the substrate, the current densities gradually became stable. Furthermore, the pH of the plating solution affected the composition of electrodeposited thin films also. Results of EDAX analysis shows nearly stoichiometric Zn/Se composition ratio for films deposited at pH 2.5.

At pH 3.0, the current density was found to be lowest. Furthermore, the as-grown films were seen to be reddish in colour (due to excess of selenium present) when observed with necked

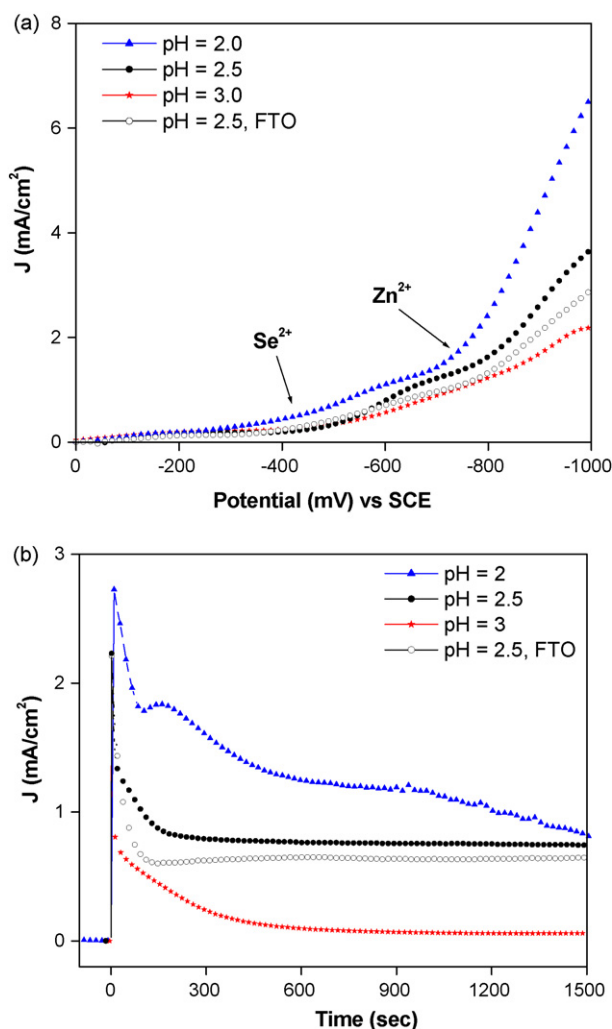


Fig. 2. (a) Linear sweep voltammogram of 0.1 M $\text{Zn}(\text{CH}_3\text{COO})_2 \cdot 2\text{H}_2\text{O} + 0.01$ M SeO_2 solution on SS (at pH 2.0, 2.5 and 3.0) and FTO (at pH 2.5) coated glass substrate (colour online). (b) Plot of variation of current density as a function of deposition time (colour online). (For interpretation of the references to colour in this figure legend, the reader is referred to the web version of the article.)

eye. In fact, the Zn/Se stoichiometric ratio was found to be 10.2/89.8.

3.2. Thickness measurement

Thickness of the film was measured with the help of surface profiler. Fig. 3(a and b) shows the thickness profile plot for ZnSe thin film deposited on SS and FTO coated glass substrate, respectively. The edge of the film is scanned in horizontal direction (1 μm). At substrate–film interface (edge of the film) there is sharp rise in vertical direction of the plot. This sharp rise at the edge of the film is attributed to the thickness of the film. From this plot the thickness of the film deposited on SS and FTO coated glass substrate is found out to be 0.761 and 1.062 μm , respectively for 60 min deposition time.

3.3. X-ray diffraction analysis

The crystallinity and orientation of the ZnSe films are determined by X-ray diffraction (XRD) using $\text{CuK}\alpha$ radiation. Fig. 4(a and b) shows the X-ray diffractogram of the ZnSe films grown on SS and FTO coated glass substrate, respectively. It is observed that the XRD pattern of the film show a most preferred orientation along

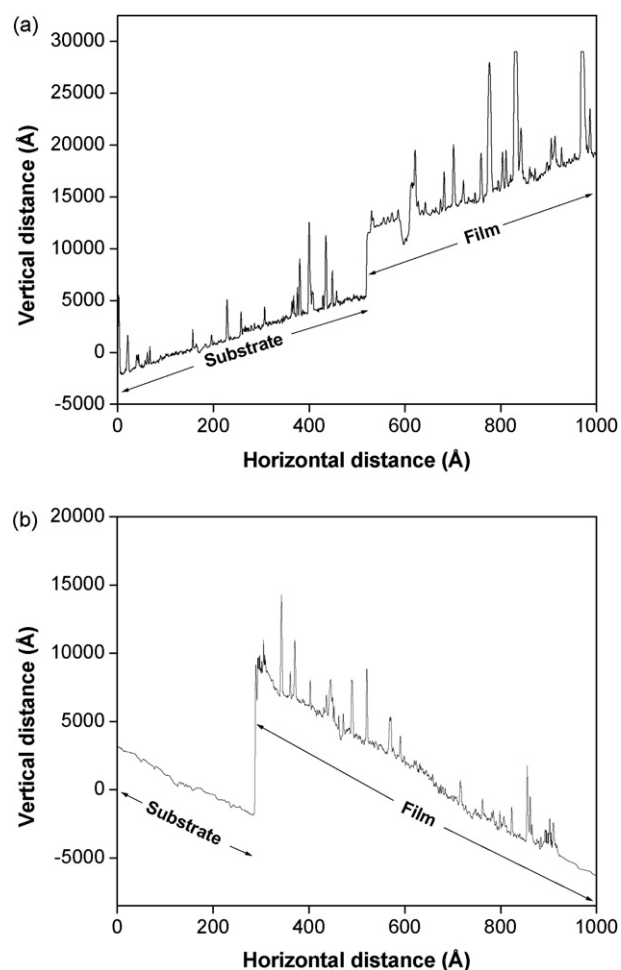


Fig. 3. Thickness profile plot for ZnSe thin film deposited on (a) SS and (b) FTO coated glass substrate.

(111) plane. The (111) direction is the close-packing direction of the zincblend structure and the deposited films are polycrystalline having a cubic zincblend structure. The diffraction peaks at $2\theta = 27.2^\circ$, 45.1° and 53.5° are attributed to (111), (220) and (311) planes, respectively of cubic ZnSe phase, which is confirmed using the standard JCPDS data card [21]. Some peaks of substrates (SS peak in Fig. 4(a) and FTO peak in Fig. 4(b)) were also observed in the XRD patterns. The various structural parameters for ZnSe thin films deposited on the SS and the FTO substrates at pH 2.5 are calculated using standard formulae and are systematically represented in Table 1.

The lattice constant (a) for plane (111) is obtained from the X-ray analysis using the following relationship for cubic crystal [22],

$$a = d\sqrt{h^2 + k^2 + l^2} \quad (6)$$

Table 1
Various structural parameters of electrodeposited ZnSe thin films.

Substrate	$2\theta_{\text{obs}} (^\circ)$	$d_{\text{obs}} (\text{Å})$	$d_{\text{std}} (\text{Å})$	(hkl)	$a (\text{Å})$
Stainless steel (SS)	27.210	3.2747	3.2729	(111)	5.6719
	45.184	2.0051	2.0046	(220)	5.6713
	53.558	1.7096	1.7093	(311)	5.6703
FTO coated glass	27.215	3.2741	3.2729	(111)	5.6709
	45.190	2.0048	2.0046	(220)	5.6706
	53.560	1.7096	1.7093	(311)	5.6702

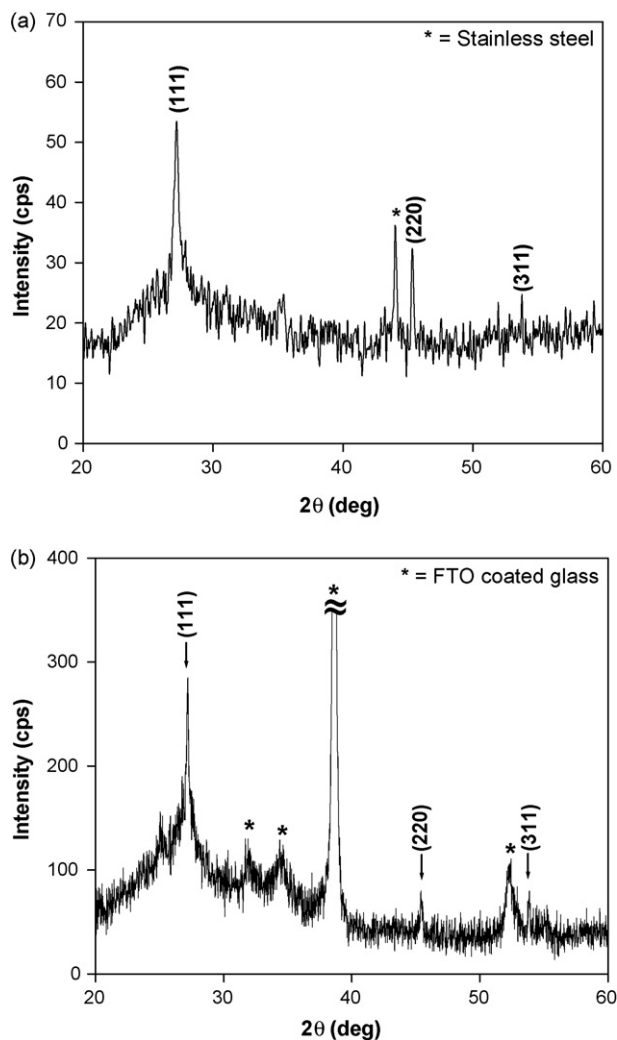


Fig. 4. XRD pattern of ZnSe thin film deposited on (a) SS and (b) FTO coated glass substrate at pH 2.5.

where h , k , l are the miller indices and ' d_{hkl} ' is the distance between the crystallographic planes. The lattice parameter calculated ($a=5.67\text{ \AA}$) matches very well with the standard value reported by other workers [23,24].

3.4. Morphological and compositional analysis

The surface morphology of electrosynthesized ZnSe thin film was investigated using SEM and AFM technique. Scanning electron microscopy has been proved to be a unique, convenient and versatile method to analyze surface morphology of a film and to determine the grain size. Fig. 5(a and b) shows the SEM images of ZnSe thin film deposited at optimized preparative parameters on the SS and the FTO substrate, respectively. From SEM images, it is observed that the as-deposited ZnSe film is uniform, without cracks with dense surface morphology covering entire substrate surface area. Films deposited on the SS substrate revealed dense morphology of irregular grains (average size $220 \pm 20\text{ nm}$). However, the films deposited on the FTO substrate revealed that grains were very small in size with no well-defined grain boundaries. The substrate morphological features, besides any epitaxial effect, vigorously define the nucleation and subsequent formation of the semiconductive layers. In addition, the substrate plays an important role in defining the surface properties like the grain distribution, porosity, etc. Hence, from the SEM micrograph of the ZnSe thin

film deposited on the FTO gives rise to extremely different morphology (porous nature) as compared to film deposited on the SS substrate (compact granular nature). Generally, semiconductor films with porous structures showed improved performance of solar cells [25]. Not only this, but for various applications like optical band pass filters [26] and high sensitive chemical sensors also require the surface to be porous in nature [27]. Therefore considering our future goal of the photovoltaic device application (as a window layer), the films deposited on the FTO substrate are better. The porous nature of the film will improve the photovoltaic performance by enhancing light trapping ability (anti-reflection coating property) [28]. Fig. 6(a and b) shows a typical two-dimensional (2D) and three-dimensional (3D) AFM image ($2\text{ }\mu\text{m} \times 2\text{ }\mu\text{m}$) of the ZnSe thin film deposited on the FTO substrate. The 2D image of the film resembles very well with the morphology of SEM micrograph (Fig. 5(b)). The surface evolution of the films showed "hill" like structures (Fig. 6(b)) which is compact and uniform covering complete substrate surface. The surface roughness was 0.48 nm . The surface roughness is unavoidable due to three-dimensional growth of the film [29].

To study stoichiometry of the film quantitative analysis was carried out using the EDAX technique. Fig. 7 shows a typical EDAX pattern for the ZnSe film deposited on the SS substrate. The elemental analysis was carried out only for Zn and Se; the average atomic percentage of Zn:Se was 42.18:57.82 showing that the sample was slightly selenium rich, which is in good agreement with the reports of Riverous et al. and Bouroushian et al. [16,19].

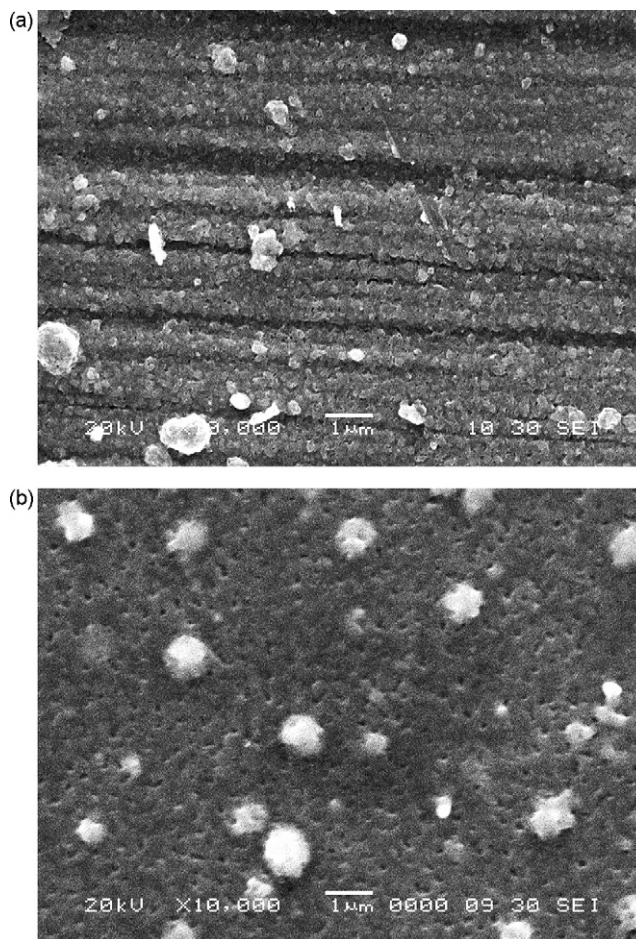


Fig. 5. SEM micrograph ZnSe thin film deposited on (a) SS and (b) FTO coated glass substrate.

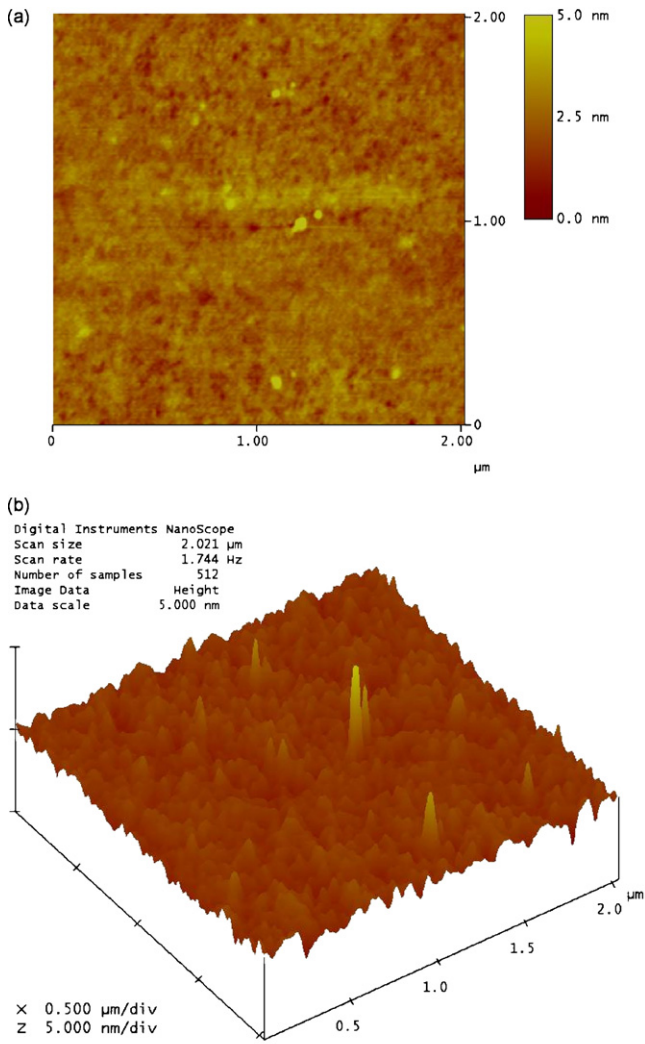


Fig. 6. (a) Two-dimensional (2D) and (b) three-dimensional (3D) AFM image of ZnSe thin film deposited on FTO coated glass substrate.

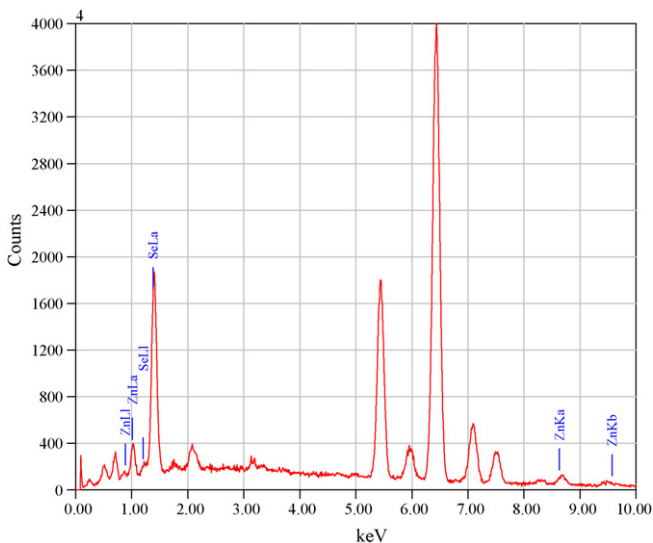


Fig. 7. Representative EDAX spectra of ZnSe thin film deposited on SS substrate.

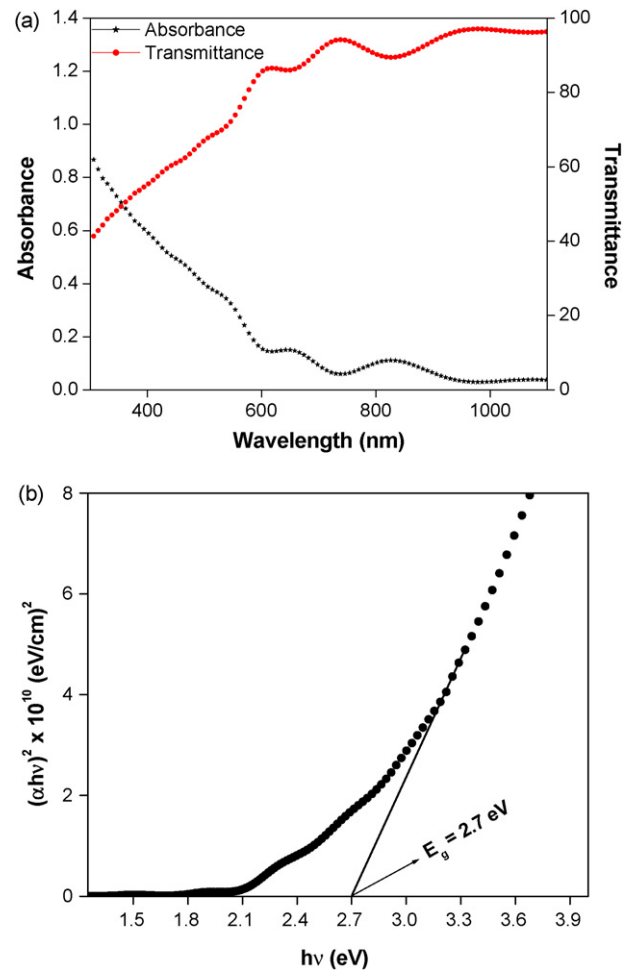


Fig. 8. Plot of variation of (a) absorbance and transmittance vs wavelength (colour online) and (b) $(\alpha hv)^2$ vs (hv) for ZnSe thin film. (For interpretation of the references to colour in this figure legend, the reader is referred to the web version of the article.)

3.5. Optical analysis

Fig. 8(a) shows transmittance and absorbance spectrum for the ZnSe thin film. The transmission is high in the red–infrared region ($>80\%$ for $\lambda > 600$ nm) and decrease to a value of 55% in the blue region (the transmission is 55.8% at 405 nm). The transmittance data was used to calculate the absorption coefficient (α) using Tauc's relation

$$\alpha hv = A(hv - E_g)^{1/2} \tag{7}$$

where hv is the photon energy, E_g is the band gap energy and A is some constant. Further, absorption coefficient (α) can be simplified as,

$$\alpha = \frac{-\ln(T)}{t} \tag{8}$$

where T is the transmittance and t is the thickness of the film. The transmittance data was used to determine the thickness and extinction coefficient [30] of the film using envelop method [31]. The thickness of the film comes out to be 1.023 μm , which is very close to the value determined with the help of surface profiler (1.062 μm). The extinction coefficient and refractive index was found out to be 0.313 and 1.65, respectively.

Fig. 8(b) shows the variation of $(\alpha hv)^2$ against (hv) for the ZnSe thin film. Extrapolating the straight-line portion of the plot of $(\alpha hv)^2$ vs (hv) for zero absorption coefficient value gives the band

gap, which is found to be 2.7 eV and is in good agreement with the value reported earlier [15].

4. Conclusions

ZnSe thin films have been successfully deposited by electrodeposition technique at room temperature. Growth kinetics of ZnSe thin films were examined by using cyclic voltammetry and chronoamperometry. XRD study revealed polycrystalline nature of the films with cubic phase. SEM and AFM micrographs show that the present films are uniform, homogeneous and well covered on the substrate. The surface morphology of the film deposited on the SS substrate looks quite different than the one deposited on FTO coated glass substrate. From the surface morphological studies we could conclude that the substrate plays a beneficial role while formation of thin layers of ZnSe on it. Compositional analysis of the film shows nearly stoichiometric film formation at pH 2.5. Further efforts will be directed to decreasing the content of excess Se by vacuum annealing. Optical characterization of the film shows the characteristic transition of semiconductive ZnSe at 2.7 eV.

Acknowledgements

The authors are thankful to The Head, Department of Physics, Dr. B.A.M. University, Aurangabad for providing laboratory facilities, Dr. D.M. Phase (UGC–DAE Consortium for Scientific Research Centre Facilities, Indore), Mr. F. Singh, Mr. P. Kulariya, Dr. A. Tripathi, Mrs. I. Sulaniya (Inter University Accelerator Center (IUAC), New Delhi) and Mr. S.S. Shinde (Common Facility Centre, Pune) for helping out in characterizing our samples. One of the authors, Ramphal Sharma wishes to thank the Korean Science and Engineering Foundation for the award of Brain pool fellowship and author Mr. Y.G. Gudage acknowledges to The Principal, Mulshi Institute of Technology and Research, Sambhave, Pune for their kind support and valuable discussion made during the research work.

References

- [1] A. Rumberg, C. Sommerhalter, M. Toplak, A. Jager-Waldau, M.C. Lux-Steiner, *Thin Solid Films* 361 (2000) 172.
- [2] T.L. Chu, S.S. Chu, G. Chen, J. Britt, C. Ferekides, C.Q. Wu, *J. Appl. Phys.* 71 (8) (1992) 3865.
- [3] T.L. Chu, S.S. Chu, *Solid State Electron* 38 (3) (1995) 533.
- [4] V. Kumar, K.L.A. Khan, G. Singh, T.P. Sharma, M. Hussain, *Appl. Surf. Sci.* 253 (2007) 3543.
- [5] G.I. Rusu, M. Diciu, C. Pirghie, E.M. Popa, *Appl. Surf. Sci.* 253 (2007) 9500.
- [6] S. Venkatachalam, D. Mangalaraj, S.K. Narayandass, *Physica B* 393 (2007) 47.
- [7] Y.R. Ryu, S. Zhu, S.W. Han, H.W. White, P.F. Miceli, H.R. Chandrasekhar, *Appl. Surf. Sci.* 127 (1998) 496.
- [8] R.B. Kale, C.D. Lokhande, R.S. Mane, S.-H. Han, *Appl. Surf. Sci.* 252 (2006) 5768.
- [9] C.D. Lokhande, P.S. Patil, A. Ennaoui, H. Tributsch, *Appl. Surf. Sci.* 123 (1998) 294.
- [10] C.A. Estrada, P.K. Nair, M.T.S. Nair, R.A. Zingaro, E.A. Meyers, *J. Electrochem. Soc.* 141 (1994) 802.
- [11] J.M. Dona, J. Herreo, *J. Electrochem. Soc.* 142 (1995) 764.
- [12] R. Chandramohan, C. Sanjiviraja, T. Mahalingam, *Phys. Stat. Sol.* 163 (1997) R11.
- [13] M. Bouroushian, T. Kosanovic, N. Spyrellis, *J. Cryst. Growth* 277 (2005) 335.
- [14] T. Kosanovic, M. Bouroushian, N. Spyrellis, *Mater. Chem. Phys.* 90 (2005) 148.
- [15] C. Natarajan, M. Sharon, C.L. Clement, M.N. Spallart, *Thin Solid Films* 237 (1994) 118.
- [16] G. Riverous, H. Gomez, R. Henriquez, R. Schreiber, R.E. Marotti, E.A. Dalchiele, *Solar Energy Mater. Solar Cells* 70 (2001) 255.
- [17] D. Gal, G. Hodes, *J. Electrochem. Soc.* 147 (2000) 1825.
- [18] D. Kaushik, M. Sharma, R.R. Singh, D.K. Gupta, R.K. Pandey, *Mater. Lett.* 60 (2006) 2994.
- [19] M. Bouroushian, T. Kosanovic, Z. Loizos, N. Spyrellis, *J. Solid State Electrochem.* 6 (2002) 272.
- [20] Y.G. Gudage, N.G. Deshpande, A.A. Sagade, S.M. Pawar, C.H. Bhosale, R. Sharma, *Bull. Mater. Sci* 30 (2007) 321.
- [21] JCPDS Card no. 37-1463.
- [22] B. Pejova, A. Tanuevski, I. Grozdanov, *J. Solid State Chem.* 177 (2004) 4785.
- [23] S. Venkatachalam, D. Mangalaraj, S.K. Narayandass, *J. Phys. D: Appl. Phys.* 39 (2006) 4777.
- [24] G.I. Rusu, V. Ciupina, M.E. Popa, G. Prodan, G.G. Rusu, C. Baban, *J. Non-Cryst. Solids* 352 (2006) 1525.
- [25] D.H. Wang, H.P. Jacobson, R. Kou, J. Tang, R.Z. Fineman, Y.F. Lu, *Chem. Mater.* 18 (2006) 4231.
- [26] P.A.C. Van, J.C. Sit, M.J. Brett, *J. Appl. Phys.* 98 (2005) 083517.
- [27] S. Virji, J. Huang, R.B. Kaner, B.H. Weiller, *Nano. Lett.* 4 (2004) 491.
- [28] W.A. Badawy, *J. Alloys Comp.* 464 (2008) 347–351.
- [29] R.B. Kale, C.D. Lokhande, *Semicond. Sci. Technol.* 20 (2005) 1.
- [30] J.C. Manificier, J. Gasiot, J.P. Fillard, *J. Phys. E* 9 (1976) 1002.
- [31] R. Swanepoel, *J. Phys. E: Sci. Instrum.* 16 (1983) 1214.